Supplemental material

Yen and Lewis, https://doi.org/10.1085/jgp.201711985

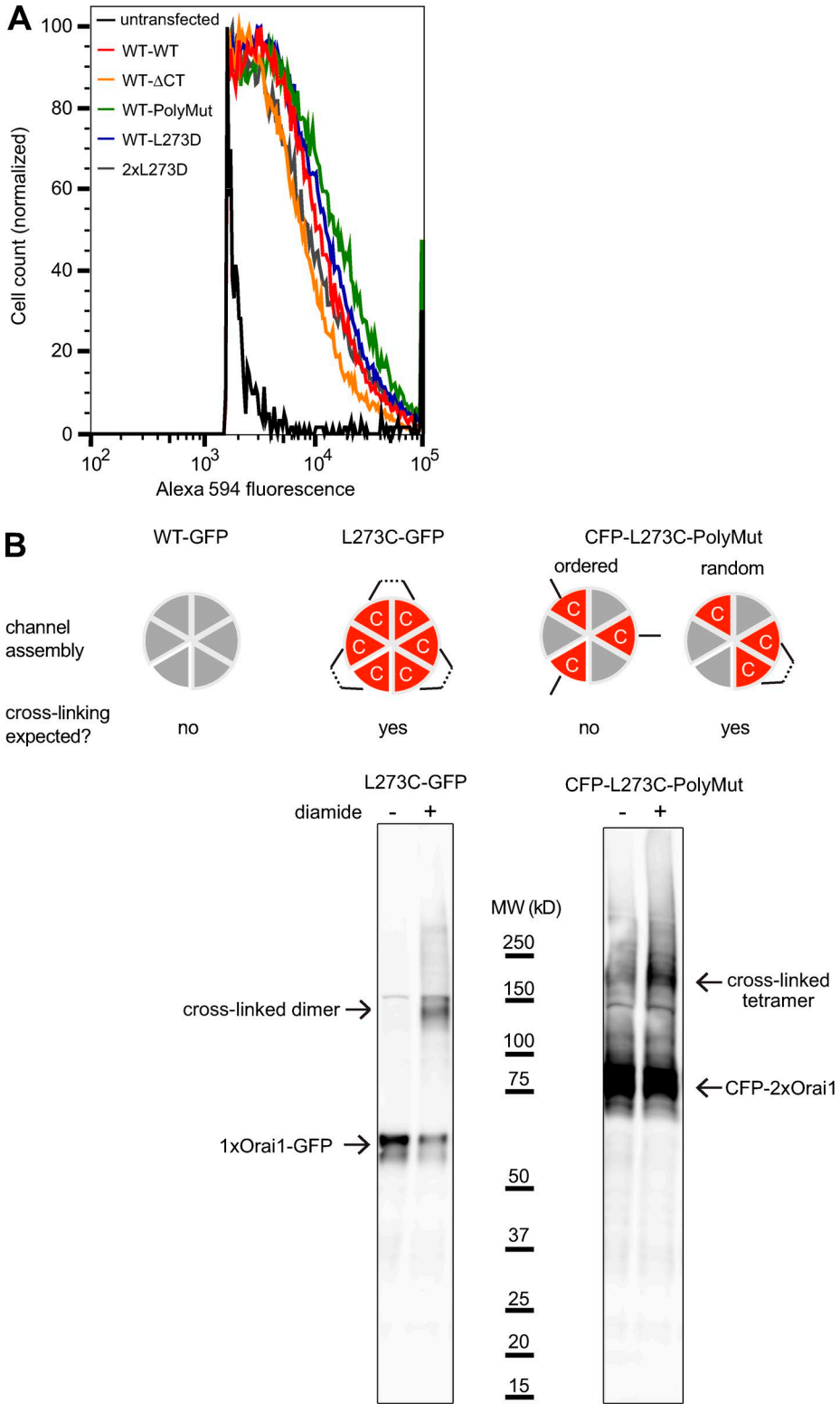

Figure S1. **Surface expression and cross-linking analysis of 2xOrai1 dimers. (A)** HEK293 cells were transfected with CFP-2xOrai1 dimer plasmid, stained with 2C1.1–Alexa 594 anti-Orai1 antibody, and analyzed by flow cytometry. Histogram shows the Alexa 594 intensity distribution of dimer-expressing (CFP-positive) cells compared with untransfected cells. **(B)** Cells transfected with monomeric Orai1(L273C)-GFP positive control or CFP-Orai1(L273C)–Orai1(PolyMut) dimer plasmid were treated with 0.25 mM diamide, lysed, and analyzed by Western blotting with anti-Orai1 antibody. As previously reported, Orai1(L273C) cross-linked in the presence of diamide to form dimers as indicated by a higher molecular weight band (Tirado-Lee et al., 2015). The L273C-PolyMut dimer was also cross-linked by diamide, indicating that a fraction of channels assemble in a random order that would place L273C Orai1 SUs adjacent to one another.

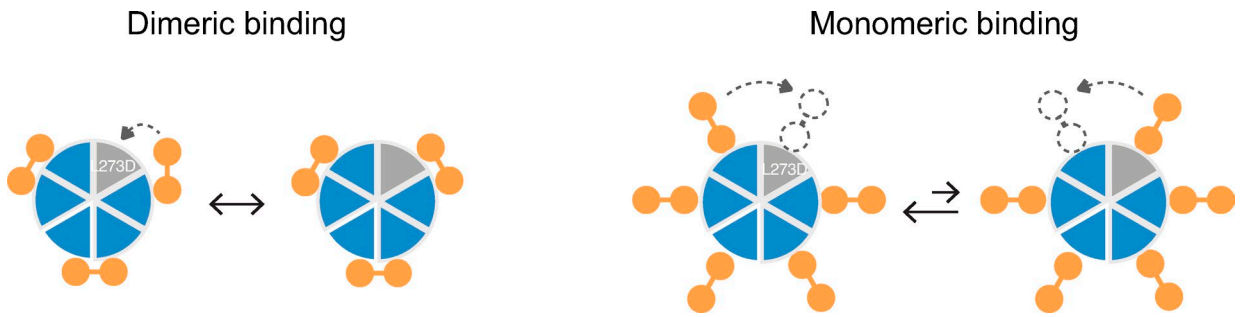

Figure S2. **Schematic of dimeric versus monomeric STIM1 binding modes.** SUs of the Orai1 hexameric channel are depicted as blue (WT) or gray (L273D) wedges. Dimeric STIM1 units are shown as linked yellow circles. Left: In a dimeric binding mode, a dimer of STIM1s binds to a pair of Orai1 SUs. Right: In a monomeric binding mode, the STIM1 dimer binds to individual Orai1 SUs. In both cases, the L273D SU enhances overall binding and current when the STIM1 binds to the neighboring WT SU, increasing the local concentration of STIM1 enough to engage the low-affinity L273D SU, either directly (dimeric mode) or after unbinding and diffusing a short distance from the WT SU (monomeric mode).

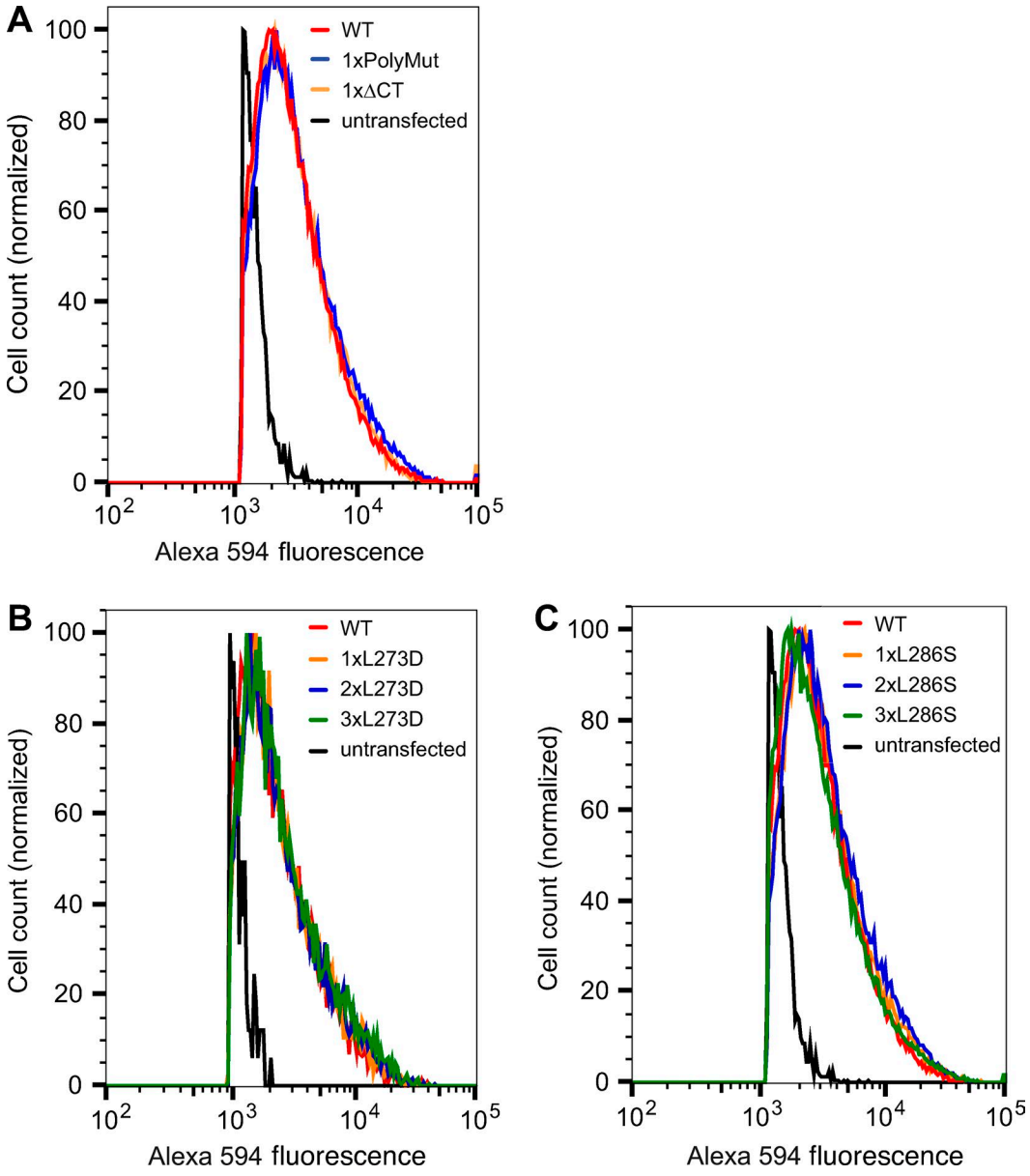

Figure S3. **Surface expression of hexameric Orai1 mutants.** HEK293 cells were transfected with GFP-labeled hexameric Orai1 plasmids, cultured as for electrophysiology experiments, stained with 2C1.1–Alexa 594, and analyzed by flow cytometry as in Fig. S1. Each histogram shows the Alexa 594 distribution of hexamer-expressing (GFP-positive) cells compared with untransfected cells. The distribution of expression levels was similar across WT, 1xPolyMut, and 1xΔCT hexamers (A); WT, 1xL273D, 2xL273D, and 3xL273D hexamers (B); and WT, 1xL286S, 2xL286S, and 3xL286S hexamers (C).

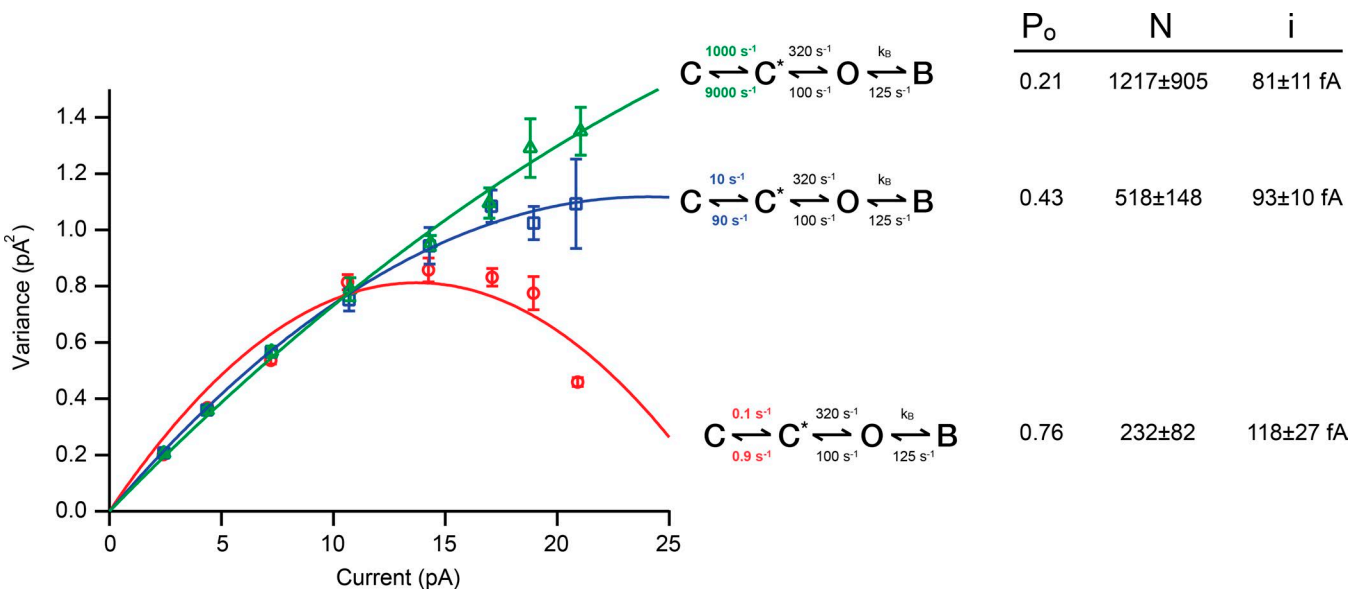

Figure S4. **Effect of closed state channel kinetics on estimating *N* and *Po* by noise analysis.** Single-channel currents were simulated for the indicated four-state model, where *C* and *C** are closed, *O* is open, and *B* is the Ca^{2+}-blocked state. 100 sweeps were generated for each model (200-ms sweeps, 200-µs sample interval, *N* = 1,000 channels, and *i* = −88 fA). The unblocking rate for Ca^{2+} from the CRAC channel (125 s^{-1}) was measured previously (Prakriya and Lewis, 2006). Ca^{2+} blocking rate constants (k_B) were adjusted to generate a range of current values, and current and variance were measured for each sweep; averages ± SEM are shown with parabolic fits as described in Fig. S4 to estimate *N*, *i*, and P_o (with 95% confidence intervals). For the unblocked channel, P_o = 0.24 for the entire kinetic scheme, and P_o = 0.76 for the $C^* \leftrightarrow O$ equilibrium. When $C \leftrightarrow C^*$ transitions are rapid (green), channels equilibrate rapidly among C states, all channels are sampled, and P_o and *N* approach their true values. As $C \leftrightarrow C^*$ transitions are slowed (blue and red), P_o increases toward the value for the $C^* \leftrightarrow O$ equilibrium and *N* declines as the sampling becomes biased toward channels closer to the open state. Single-channel current simulations were performed using Patch Machine (V. Avodnin and T. Hoshi, University of Pennsylvania, Philadelphia, PA).

References

Prakriya, M., and R.S. Lewis. 2006. Regulation of CRAC channel activity by recruitment of silent channels to a high open-probability gating mode. *J. Gen. Physiol.* 128:373–386. https://doi.org/10.1085/jgp.200609588

Tirado-Lee, L., M. Yamashita, and M. Prakriya. 2015. Conformational changes in the Orai1 C-terminus evoked by STIM1 binding. *PLoS One*. 10:e0128622. https://doi.org/10.1371/journal.pone.0128622